



The important but weakening maize yield benefit of grain filling prolongation in the US Midwest

Peng Zhu¹  | Zhenong Jin^{1,2}  | Qianlai Zhuang^{1,3} | Philippe Ciais⁴ | Carl Bernacchi^{5,6} | Xuhui Wang⁴ | David Makowski⁷ | David Lobell²

¹Department of Earth, Atmospheric, and Planetary Sciences, Purdue University, West Lafayette, Indiana

²Department of Earth System Science, Center on Food Security and the Environment, Stanford University, Stanford, California

³Department of Agronomy, Purdue University, West Lafayette, Indiana

⁴Laboratoire des Sciences du Climat et de l'Environnement (LSCE), CEA CNRS UVSQ, Gif-sur-Yvette, France

⁵Department of Plant Biology, University of Illinois at Urbana-Champaign, Urbana, Illinois

⁶Global Change and Photosynthesis Research Unit, USDA-ARS, Urbana, Illinois

⁷UMR 211 Agronomie INRA, Agroparistech, Université Paris-Saclay, Thiverval-Grignon, France

Correspondence

Qianlai Zhuang, Department of Earth, Atmospheric, and Planetary Sciences, Purdue University, West Lafayette, IN.
Email: qzhuang@purdue.edu

Funding information

NSF, Grant/Award Number: IIS-1027955; NASA LCLUC, Grant/Award Number: NNX09AI26G

Abstract

A better understanding of recent crop yield trends is necessary for improving the yield and maintaining food security. Several possible mechanisms have been investigated recently in order to explain the steady growth in maize yield over the US Corn Belt, but a substantial fraction of the increasing trend remains elusive. In this study, trends in grain filling period (GFP) were identified and their relations with maize yield increase were further analyzed. Using satellite data from 2000 to 2015, an average lengthening of GFP of 0.37 days per year was found over the region, which probably results from variety renewal. Statistical analysis suggests that longer GFP accounted for roughly one-quarter (23%) of the yield increase trend by promoting kernel dry matter accumulation, yet had less yield benefit in hotter counties. Both official survey data and crop model simulations estimated a similar contribution of GFP trend to yield. If growing degree days that determines the GFP continues to prolong at the current rate for the next 50 years, yield reduction will be lessened with 25% and 18% longer GFP under Representative Concentration Pathway 2.6 (RCP 2.6) and RCP 6.0, respectively. However, this level of progress is insufficient to offset yield losses in future climates, because drought and heat stress during the GFP will become more prevalent and severe. This study highlights the need to devise multiple effective adaptation strategies to withstand the upcoming challenges in food security.

KEYWORDS

crop growth stages, crop model, food security, global warming, Maize grain filling prolongation, satellite data, US Midwest, yield benefit

1 | INTRODUCTION

Agricultural systems in many regions may be negatively impacted by increasing temperature especially when accounting for the nonlinear effect of climate extremes such as heat waves and droughts (Porter & Semenov, 2005; Rattalino Edreira & Otegui, 2013; Sánchez, Rasmussen, & Porter, 2014; Schlenker & Roberts, 2009), which are predicted to become increasingly frequent in a warmer climate. Higher-than-optimal temperature negatively impacts maize yield through affecting reproductive structures (Siebers et al., 2015, 2017),

decreasing the Rubisco activation (Crafts-Brandner, 2002) and increasing water stress (Lobell et al., 2013). Thus, to maintain or potentially increase productivity, agricultural systems must adapt to upcoming warmer and more extreme climates.

As the world's largest producer of maize, the United States has seen a steady increase in maize yield since the 1950s through improvements in agronomic practices, genetic technology and favorable growing conditions despite interannual yield variability related to hot and dry summers (USDA, 2015). Several possible mechanisms have been investigated in order to understand this increasing trend

in yields, including: expansion of more heat-tolerant cultivars (Driedonks, Rieu, & Vriezen, 2016), delayed foliar senescence or stay-green traits (Thomas & Ougham, 2014), new cultivars adapted to higher sowing density (Duvick, 2005; Tollenaar & Wu, 1999), development of pest resistant maize cultivars through genetically engineering (NRC, 2010), enhanced water use efficiency under rising atmospheric CO₂ (Jin, Ainsworth, Leakey, & Lobell, 2018; Lobell & Field, 2008), and increase in accumulated solar radiation during the postflowering phase (Tollenaar, Fridgen, Tyagi, Stackhouse, & Kumudini, 2017). A drought sensitivity analysis over the US Midwest based on field maize yield data showed, however, higher sowing density brought about side effect that field maize yield sensitivity to water stress became increased (Lobell et al., 2014). In this context, it is necessary to understand the response of maize yield in farmers' fields to climate variation over time and thereby allowing crops more effectively to adapt to the future climate change.

Crop phenological development is essential for agricultural management practices (Irmak, Haman, & Bastug, 2000), and reflects the combined effect of climate exposure and plant physiological traits (McMaster, 2005). Specifically, this study focused on GFP, a critical kernel development stage when plant growth and grain formation is sensitive to stress (Badu-Apraku, Hunter, & Tollenaar, 1983; Çakir, 2004; Cheikh & Jones, 1994). In addition, because there is a tight positive correlation between the grain filling length (GFL) and the final crop yield (Badu-Apraku et al., 1983; Tollenaar et al., 2017), characterizing recent trends in GFL may also help explain yield trends.

Satellite remote sensing observations such as the vegetation index derived from moderate-resolution imaging spectroradiometer (MODIS) reflectance data provide the opportunity to characterize the regional-scale spatiotemporal patterns of field crop growth status information, in particular phenological transition dates (Sakamoto et al., 2010). We used this long-term satellite data to generate spatially explicit maize phenological date fields. Maize phenological

information was then integrated with a crop model to understand the relationship between GFP trend and yield increase in the historic period. Finally, the implication of longer maturity variety for sustaining maize production under future climate scenarios was investigated.

2 | MATERIALS AND METHODS

In this study, 8-day Wide Dynamic Range Vegetation Index (WDRVI) derived from MODIS reflectance data (MOD09Q1 and MYD09Q1) from 2000 to 2015 was used to map trends in maize phenology in Illinois, Indiana, Iowa, Nebraska across the US Midwest, which collectively account for half of the total US maize production. Maize yield keeps growing across the four states at the rate of 1.4% per year during this period (Figure 1). To extract maize phenology, shape model fitting (SMF) has been shown as an effective approach and was validated at both site and state level (Sakamoto, Gitelson, & Arkebauer, 2014; Sakamoto et al., 2010; Zeng et al., 2016). On the other hand, threshold-based methods can be used to extract the starting and ending of growing season more flexibly. Thus, we developed and implemented a hybrid method combining SMF and threshold-based analysis to generate 8 million samples of maize phenological date from MODIS WDRVI data at 250 × 250 m spatial resolution from 2000 to 2015.

2.1 | Satellite data

In this study, the 8-day time series of 250 m daily surface reflectance MODIS data on board Earth Observing System (EOS) Terra and Aqua satellite platforms: MOD09Q1 (2000–2015) and MYD09Q1 (2002–2015) Collection 6, was used. Four tiles MODIS data (h10v04, h11v04, h10v05, h11v05) covering the study area (4 states: Indiana, Illinois, Iowa, Nebraska) were downloaded from NASA Land Processes Distributed Active Archive Center. Although

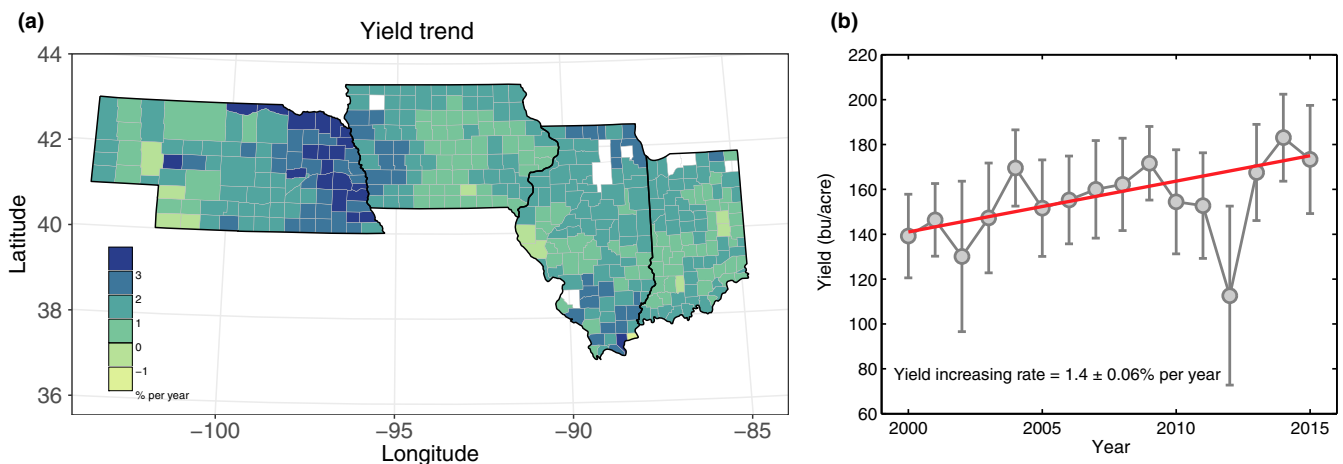


FIGURE 1 (a) Trends in maize yield for each county, where the empty counties mean that county has <12 years available data. (b) Mean maize yield increasing rate for all counties. The error bars indicate the spatial variation of maize yield for all counties

the daily satellite observations can better capture the phenological phase transition during maize growth, the 8-day composite products in MOD09Q1 and MYD09Q1 were selected to minimize the impact of clouds and haze. Generally, the MODIS 8-day composite products were systematically corrected for the effects of aerosol light scattering (Vermote & Vermeulen, 1999). Meanwhile, the constrained view-angle maximum value composite method guarantees the quality of surface spectral reflectance data for each 8-day period (Huete et al., 2002). Both 250 m MOD09Q1 and MYD09Q1 data consist of red (R) and near-infrared (NIR) bands with an actual spatial resolution of 231.7 m. Here a scaled WDRVI (Wide Dynamic Range Vegetation Index), generated by combining Terra and Aqua observations, is used to monitor the growing status of maize plants (Zeng et al., 2016), because WDRVI is supposed to have a better performance in characterizing seasonal biomass dynamics than normalized difference vegetation index (NDVI), which is often saturated for dense vegetation and a linear relationship was identified between WDRVI and the green leaf area index (LAI) of both maize and soybean (Gitelson, 2004; Gitelson, Schalles, & Hladik, 2007). The scaled WDRVI is calculated with the following equation:

$$\text{WDRVI} = 100 * \frac{[(\alpha - 1) + (\alpha + 1) \times \text{NDVI}]}{[(\alpha + 1) + (\alpha - 1) \times \text{NDVI}]} \quad (1)$$

$$\text{NDVI} = (\rho_{\text{NIR}} - \rho_{\text{red}}) / (\rho_{\text{NIR}} + \rho_{\text{red}}) \quad (2)$$

Where ρ_{red} and ρ_{NIR} are the MODIS surface reflectance in the red and NIR bands, respectively. A comparison of multiple vegetation indexes indicates WDRVI with $\alpha = 0.1$ showed a strong linear correlation with corn green LAI (Guindin-Garcia, Gitelson, Arkebauer, Shanahan, & Weiss, 2012). Here we also set α as 0.1 for WDRVI calculation. Before WDRVI calculation, the reflectance data were quality-filtered using the band quality control flags. Only the data passing the highest quality control test are retained.

2.2 | Crop location information

A cropland dynamic layer (CDL) spanning from 2000 to 2015 generated by USDA/NASS was used to be as maize mask (The time span of NASS-CDL for Nebraska is from 2001 to 2015). The spatial resolution of the original products of NASS-CDL varied from year to year due to different satellite data being used. The satellite datasets used to generate NASS-CDL over 2000–2005 and 2010–2015 were obtained from Landsat/TM with 30 m resolution. Those used to generate NASS-CDL over 2006–2009 were obtained from Resourcesat-1/AWiFS with 56 m resolution. The CDL data were firstly projected to MODIS sinusoidal projection and then aggregated to 231.7 m. We only extracted the phenological information over the MODIS pixels with the corresponding maize fraction surpassing 80% determined by CDL aggregation, which can thus suppress the mixing effect of other vegetation types like grasses and soybean. The classification errors in the CDL data might mix noncrops signal into the

WDRVI calculation. However, previous study showed that the influence of classification errors on maize phenological extraction can be minimized at regional scale (Sakamoto et al., 2014), especially when a high threshold value (here it is 80%) was applied to filter mixing pixels.

2.3 | Maize phenology and yield statistics data

USDA/NASS surveys crop progress and condition based on questionnaires and publishes percent complete (area ratio) of crop fields that have either reached or completed a specific phenological stage, on Agricultural Statistics Districts (ASD) or state level, in a weekly report called the Crop Progress Report (CPR). The state level phenology information is available in the USDA/NASS Quick Stats 2.0 database. The weekly reported area ratios were interpolated using sigmoid function. The target phenological stages (emerged, silking, dent, and mature stages) were then determined as the date when the interpolated area ratio reached 50% on a state level (Tollenaar et al., 2017). The phenological dates from CPR were used as a reference to evaluate the MODIS-based estimations.

The county-level corn grain yield data covering the four states (IL, IN, IA, NE) were obtained from the Quick Stats 2.0 database. The selected data period was from 2000 to 2015. The unit system for corn grain yield is bushel per acre (bu/ac).

2.4 | Climate data

Daily precipitation, minimum and maximum temperatures, and relative humidity data at 4 km resolution were obtained from University of Idaho Gridded Surface Meteorological Data (Abatzoglou, 2013) (<http://metdata.northwestknowledge.net/>). It is a gridded product covering the US continent and spanning from 1979 to 2016. This dataset is created by combining attributes of two datasets: temporally rich data from the North American Land Data Assimilation System Phase 2 (Mitchell, 2004) (NLDAS-2), and spatially rich data from the Parameter-elevation Regressions on Independent Slopes Model (Daly et al., 2008; PRISM). After validated using extensive network of weather stations across the United States, this dataset is proved to be suitable for landscape-scale ecological model. To be consistent with the climate data resolution, MODIS-derived maize phenology information is aggregated to 4 km by averaging all available maize phenological date. Then the climate variables like mean temperature, mean VPD and mean precipitation during the vegetative period, grain filling period, and total growth period are estimated by integrating daily climate data over the corresponding period according to MODIS-derived phase starting and ending date. VPD is estimated from relative humidity and temperature data.

Here GDD, a commonly used metric as the cumulative thermal requirement for a crop having experienced over the growing season for maize, is calculated from daily temperature values. It is defined as the sum of all daily average temperatures over the growing season in excess of 8°C. A base temperature of 8°C and a maximum temperature of 35°C for maize were used (Kiniry & Bonhomme,

1991). Specifically, GDDcrit was used to refer to the GDD requirement from start grain filling to maturity.

2.5 | Maize growing phase extraction

A shape model fitting (SMF; Figure 2), which represents the general pattern of corn growth characterized by time-series WDRVI, was created using a similar procedure as previous study (Sakamoto et al., 2010). The shape model was defined by averaging 10 years (2001–2010) of 8 days WDRVI observations from the irrigated continuous corn field at Mead, Nebraska operated by the University of Nebraska Agricultural Research and Development Center. Then, the shape model was geometrically scaled and fitted to 8-day time-series WDRVI data using the following equation:

$$h(x) = yscale \times \{g(xscale \times (x + tshift))\}, \quad (3)$$

where the function $g(x)$ refers to the preliminarily defined shape model function and x refers to WDRVI acquiring date. The function $h(x)$ is transformed from the shape model $g(x)$ in time- and VI-axis directions with the scaling parameters $xscale$, $yscale$, and $tshift$. The scaling parameters were optimally estimated using “fminsearch” function in Matlab R2015b to minimize the discrepancy between the scaled shape model $h(x)$ and the WDRVI data. Here the root mean square error (RMSE) between the scaled shape model $h(x)$ and the WDRVI data is used to quantify the discrepancy. The dates of these key phenological stages, including emerged, silking, dent, and mature date, were determined from satellite data by optimizing the dates of emerged, silking, dent, and mature stages, given the predefined dates. Dent stage is about 35–42 days after silking when “milk line”

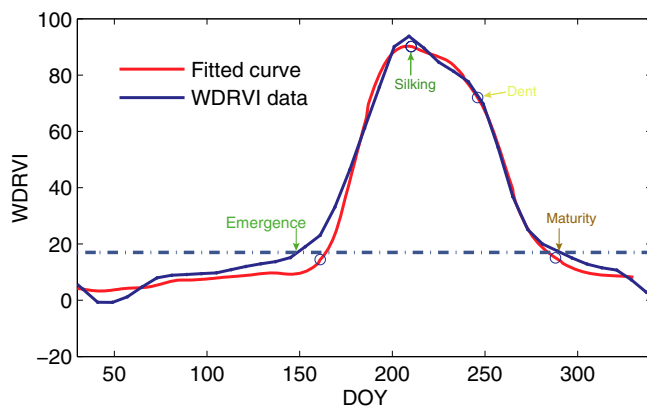


FIGURE 2 The procedure of hybrid maize phenological extraction by merging shape model fitting and threshold-based method. The blue line is the spline approach smoothed WDRVI time-series data and the red line is the scaled shape model fitting and the dashed blue line indicates the threshold, which is set as 18 based on trials when compared with the NASS reported emergence and maturity date for four states. The circle on red curve indicates the phenological date determined by shape model fitting. Here the silking and dent dates were determined by shape model fitting and the emergence and maturity date were determined by the threshold

gets close to the dent end of the kernel. Maturity date is about 55–65 days after silking and kernel dry weight reaches its maximum (Abendroth, Elmore, Boyer, & Marlay, 2011). In the original study (Sakamoto et al., 2010), the predefined dates were empirically determined based on the ground-based phenology observations and were set as 150, 200, 240, and 265 day of year of the reference growing season, respectively. These parameters are also used in this study.

Although the previous study showed SMF had a good estimation of corn phenology at site and state level with RMSE of maize phenological stage estimation at ASD-level ranging from 1.6 (silking date) to 5.6 days (dent date; Zeng et al., 2016), there is an inevitable problem in this method that the linear scaling strategy with only two parameters ($xscale$ and $tshift$) is too stiff and leads to identical trends in the four critical phenological dates. However, the US maize plants seems to have different or even opposite temporal shifts in different phenological dates as reported by Sacks and Kucharik (2011) like an advance in planting and emergence date while delay in maturity date during 1981–2005. Thus, a more flexible way to characterize the different trends in the four phenological dates is needed.

Among the numerous methods for deriving seasonal parameters from the time-series vegetation index, the threshold method, which assumes that a specific phenology will start when the vegetation index value exceeds a threshold, is widely used because it generally keeps dates within a certain reasonable range and can achieve relatively high accuracies. In general, threshold is usually selected based on crop types. In this study, the WDRVI of 18 is set as threshold based on trials when comparing the estimation with NASS reported emergence date and maturity date for four states. We used a hybrid method by merging the advantage of SMF in extracting the silking and dent dates and the threshold method in extracting the growing start (emergence) and ending (maturity) date (Figure 2). Furthermore, SMF was restricted to only fit WDRVI curve for a specific range, where WDRVI is above its 40% peak value, so the estimated parameters are mainly relevant to the silking and denting phenological information. Before applying the threshold method, the WDRVI curve is firstly smoothed using a robust smoothing-spline approach to reduce the signal noise (Keenan et al., 2014). To minimize the impact of maize pixels contaminated by clouds, cloud shadow and aerosol loading, a 3×3 windows is used to filter the data. In each 3×3 windows, only those with more than four maize pixels were selected for phenology extraction, so there were multiple observational vegetation index data to constrain the optimization model, which can thus improve the stability of parameters estimation. In addition, the searching boundary for the scaling parameter $yscale$ and $xscale$ was empirically set as [0.4, 1.8] to ensure the extracted phenological date within a reasonable range. Finally, approximate 8 million grids containing the four critical phenological date over 16 years were retrieved. When the MODIS extracted emergence date was aggregated to the state level and compared with the NASS CPR, we found a systematic bias in emergence dates that MODIS estimated emergence dates were 7.6 days later than the NASS report date. This systematic bias might result from the selection of WDRVI threshold. Then this systematic bias was deducted from the

TABLE 1 RMSE (days) of four phenological stages estimation over four states

State	Emergence	Silking	Dent	Maturity
Illinois	4.0	1.9	2.8	3.4
Indiana	4.2	2.2	4.0	3.2
Iowa	2.9	4.3	3.3	3.6
Nebraska	3.1	1.6	4.4	3.0

MODIS-derived emergence date before comparison. Nevertheless, the bias will not influence the estimation of grain filling starting and ending date. The state level comparisons show a good agreement for the four key phenological stages with the RMSE ranging from 1.6 (silking date) to 4.4 days (dent date; Table 1).

Finally, the GFP and grain filling GDD_{crit} trend was analyzed in 4 km grid cell to keep consistent with the spatial resolution of climate data. This larger grid size than the original resolution of MODIS data (250 m) brings more phenological samples for trend analysis, thus a stronger statistical inference can be made.

2.6 | Yield stability and GFP

Generalized additive regression model (GAM), an effective and flexible method to characterize nonlinear effects of explanatory variables, was used here to explore the relationship between yield stability and GFP. Coefficient of variation and standard deviation of county yield over time were alternatively used to represent the temporal stability of maize yield. The model was constructed based on R package “mgcv” (Wood, 2006). The spline method was used as the smooth term. In addition to GFP, climatic variables including multiyear mean precipitation, mean daily temperature, and vapor pressure deficit (VPD) during GFP over 2000–2015 were also selected as the covariates. Both county level GFP and the trends in GFP were alternately used as the explanatory variables, so the influence of the longer GFP in space and GFP extension over time on yield stability was explored.

2.7 | Crop model simulations

An agricultural system modeling platform APSIM version 7.7 is used here to simulate the benefit of GFP extension under future climate. APSIM can simulate a number of crops under different climatic and management conditions, and hence is used worldwide to address a range of research questions related to cropping systems (Holzworth et al., 2014). In particular, maize is simulated by the APSIM-Maize module. The APSIM-Maize module is inherited from the CERESMaize, with some modifications on the stress representation, biomass accumulation and phenological development (Hammer et al., 2010). This flexible process-based model allows us to separately estimate the yield benefit of agronomic practices like the cultivar shift indicated by higher thermal time requirement during grain filling.

The MODIS data showed both the grain filling GDD_{crit} and GFP increased, suggesting the GFP extension is likely to be associated with variety change, such as the adoption of longer maturity variety. We designed three simulations to explore the contribution of GFP extension to recent decades yield increase. All the simulations were forced with University of Idaho Gridded Surface Meteorological Data from 2000 to 2015. The parameter in APSIM, phase_tt (start_to_end_grain), defining the GDD requirement from start grain filling to maturity was increased to drive a prolonged GFP to emulate the adoption of longer maturity variety over this period. Simulation sim1 is the control with no increase in variety GDD_{crit}; simulation sim2 sets an increase in variety GDD_{crit} by 0.65% per year which characterized the observed increasing rate in all counties; simulation sim3 sets an increase in GDD_{crit} by 0.82% per year which represented the observed increasing rate in GFP prolonged counties. The soil parameters, like soil hydraulic properties and soil organic matter fractions were extracted from the State Soil Geographic (STATSGO) database, as collected by the National Cooperative Soil Survey over the course of a century. For each simulation grid, the soil information was queried through R package “soil DB” (<http://ncss-tech.github.io/AQP/>). Management information like planting density and fertilizer application amount was taken from the USDA NASS survey report at state level. Crop sowing date was derived from the Crop Calendar Dataset (Sacks, Deryng, Foley, & Ramanakutty, 2010). We used generic maize hybrids (“B_110”) provided by APSIM version 7.7 to run the simulation.

To investigate the yield benefit of longer GFP until 2060–2070, we constructed two simulations for climate forcing data from historic (2000–2015) period and two future climate scenarios (RCP2.6 and RCP6.0), respectively: one is the control simulation, where the maize GDD_{crit} was set as a constant using generic cultivar parameters (“B_110”); the other one is the GFP prolonged simulation, where GDD_{crit} was increased by 0.82% per year to be consistent with the current advance in maize cultivar based on historical MODIS image analysis. For the historic period simulation, the climate forcing data during 2000–2015 were recycled until 2070. For the future climate scenarios, three climate forcing data were used to account for the climate model uncertainty in global temperature: Institute Pierre Simon Laplace CM5A Earth system model (IPSL-CM5A-LR), Geophysical Fluid Dynamics Laboratory Earth System Model with Generalized Ocean Layer Dynamics component (GFDL-ESG2G) and the Hadley Centre Global Environment Model, version 2-Earth System (HadGEM2-ES). As a C₄ plant, maize plants loss less water in response to future enriched atmospheric CO₂, which is modeled by enhanced transpiration efficiency in APSIM. The CO₂ concentration is set as 380 ppm for the historic simulation while increased to follow the concentration trajectory defined in RCP2.6 and RCP6.0 (Meinshausen et al., 2011). The soil parameters and management information here followed the previous simulations sim1 (sim2, sim3). Then yield increasing rate in 2060–2070 is calculated by (yield with prolonged GFP–yield in control simulation)/(yield in control simulation) with three climate forcing data: historic period, RCP2.6 and RCP6.0.

2.8 | Conceptual model of GFP trend analysis

GDD during GFP can be generally written as:

$$\text{GDD}_8^{35} = \int_{\text{silking}}^{\text{maturity}} \text{DD}_t, \text{DD}_t = \begin{cases} 0, & \text{when } T_{\text{mean}} < 8 \\ T_{\text{mean}} - 8, & \text{when } 8 \leq T_{\text{mean}} < 35 \\ 27, & \text{when } T_{\text{mean}} \geq 35 \end{cases} \quad (4)$$

8, 35 means the lower and upper bounds of daily mean temperature (T_{mean}) to calculate GDD. As most of T_{mean} is within this range, it can be approximately written as:

$$\text{GDD}_8^{35} \approx \text{GFP} \cdot (T_{\text{mean}} - 8) \quad (5)$$

Then the GFP trend can be rearranged as:

$$\frac{d\text{GFP}}{\text{GFP} \cdot dt} \approx \frac{d\text{GDD}}{\text{GDD} \cdot dt} - \frac{d(T_{\text{mean}} - 8)}{(T_{\text{mean}} - 8) \cdot dt} \quad (6)$$

So GFP trend ($\frac{d\text{GFP}}{\text{GFP} \cdot dt}$) can be approximately estimated by GDD trend minus T_{mean} trend. As T_{mean} trend is very small (Supporting Information Figure S4), GFP trend is mostly driven by GDD trend.

2.9 | Yield benefit analysis using statistical method

We conducted a panel analysis to quantify the statistical contribution of increasing GFP to the observed increase in maize yield. A linear model considering the fixed effects in each year and county was used:

$$\log(\text{Yield}_{i,t}) = \beta_1 * \text{GFP}_{i,t} + \text{Year}_t + \text{County}_i + \varepsilon_{i,t} \quad (7)$$

where Year_t and County_i specify independent intercept of each year and county.

3 | RESULTS AND DISCUSSION

The verification at state level showed a good agreement between MODIS-derived maize phenology and the National Agricultural Statistics Service (NASS) reported state mean phenological dates for the four key maize growth stages of emergence (late May), silking (Middle July), dent (late August), and maturity (late September; Figure 3). The root mean square error (RMSE) of the four phenological dates estimated over the four states ranged from 1.6 days (silking date in Nebraska) to 4.4 days (dent date in Nebraska Table 1). The duration between emergence and maturity is used to represent maize total growth period, and the duration between silking and maturity dates is used to define the GFP. Across the four states, GFP generally starts from around day of year (DOY) 200 and ends by DOY 260 but varied interannually (Figure 3).

Grain filling period trend was analyzed on a 4km grid to keep consistent with the spatial resolution of climate data (Abatzoglou, 2013). We found there were significant trends of maize phenology, with silking dates becoming earlier in 61% of the pixels and more pixels (84%) exhibiting a later maturity date (Supporting Information

Figure S2). This resulted in a significant extension of the GFP over 81% of the pixels during the 16-year analysis (Supporting Information Figure S2). This trend of GFP obtained from satellite data is similar to NASS reports when aggregated to state level (Figure 4). This is also in line with the study over the US Corn Belt from Sacks and Kucharik (Sacks & Kucharik, 2011) that was conducted for the earlier period of 1981-2005 based on NASS state reports.

The spatial variation of the GFP trends shows increasing trends in most Midwest areas and decreasing trends in drier areas like western Nebraska (Figure 5a). The spatial mean of the GFP trends across the four states is 0.37 days per year with interquartile values ranging from 0.09 to 0.68 (Figure 5b). When aggregated to the county level, 79% of the counties exhibit a significant increase in GFP (Figure 5a). As the longer GFP might be a result of increased variety thermal time accumulation, we also looked into growing degree days (GDD). GDD is a commonly used metric to measure thermal time accumulation of crops and the critical threshold GDD_{crit} at which GFP is fulfilled is an important physiological trait of maize cultivars. The GDD_{crit} calculated from satellite and climate data shows trends that have a similar spatial structure than the GFP trends, with a mean rate of increase of 0.65% per year (Figure 5c,d). The small warming trend observed in the study area (Supporting Information Figure S4) would have shortened GFP (Egli, 2004), if GDD_{crit} keeps constant. Thus the observed longer GFP is likely to be associated with variety shifts, marked by the concurrently increasing GDD_{crit} . As GDD_{crit} reflects the thermal time requirement of a specific cultivar to achieve grain filling, the increasing GDD_{crit} over time (Figure 5c) and the higher GDD requirement from emergence to maturity in south counties with warmer temperature (Figure 6 and Supporting Information Figure S5) suggest that farmers have switched to use longer maturity cultivars to compensate for the negative impact of warmer temperatures which otherwise shorten the overall growing season length and the GFP (Çakir, 2004; Dwyer, Ma, Evenson, & Hamilton, 1994; Egli, 2004; Sacks & Kucharik, 2011).

Evidence from agronomical research shows that extended GFP contributes a higher yield by providing more time to translocate photosynthates to kernels (Crosbie & Mock, 1981; Wang, Kang, & Moreno, 1999). With Equation 7, the estimated yield benefit β_1 (% per day) defining the sensitivity of yield to GFP is $0.86 \pm 0.03\%$ (\pm standard error, SE), indicating that one additional day of GFP increased maize yield on average by 0.86%. According to this empirical relationship and the estimated total yield trend (1.4% per year), the lengthening of GFP observed in the MODIS data is inferred to have contributed to $23 \pm 0.7\%$ (\pm SE) of the maize yield trend for all of the studied counties (Figure 7a). This contribution was computed as:

$$\text{Contribution} = \beta_1 \times \text{GFP increasing trend} / \text{Yield increasing trend} \quad (8)$$

Equation 8 was also applied to the NASS reported maize phenological data at state level. In this application, the fixed effect term County_i for each county was replaced with the state fixed effect State_s , and the estimated value of β_1 was slightly higher ($1.08 \pm 0.18\%$ per days) compared to the above estimation (Figure 7a). Given the mean GFP trend (0.43 ± 0.12 days per year),

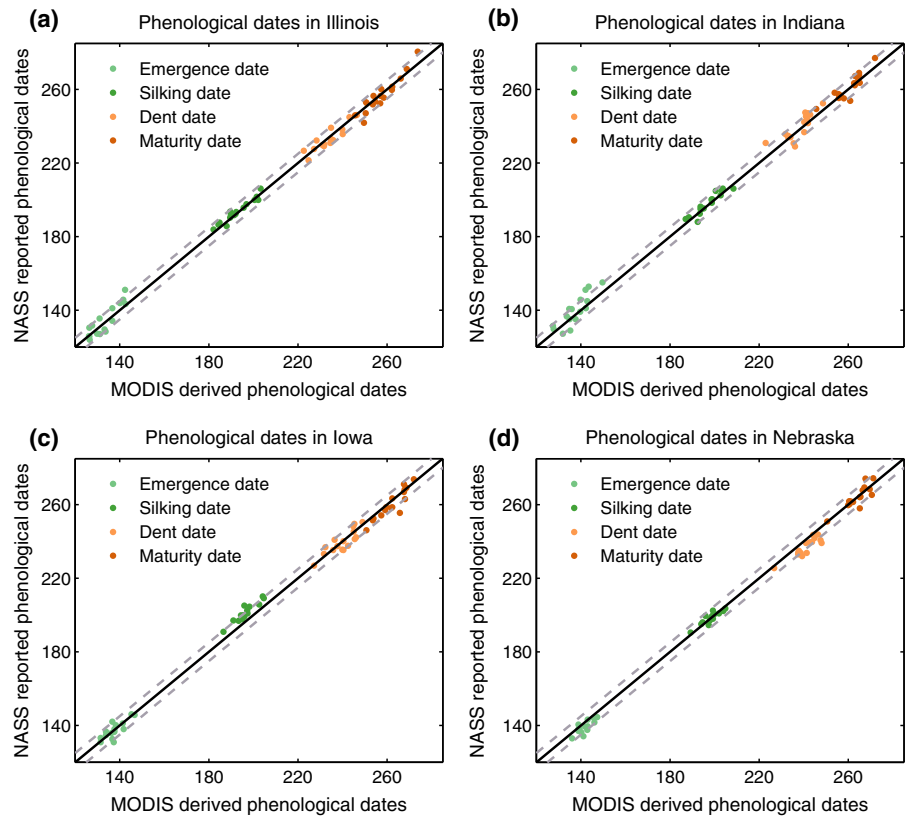


FIGURE 3 Comparison of maize phenological dates between NASS statistical data and MODIS-derived estimation aggregated over state level. The two dashed lines in each figure define the region where the errors between MODIS-derived estimation and NASS statistical data are less than 5 days

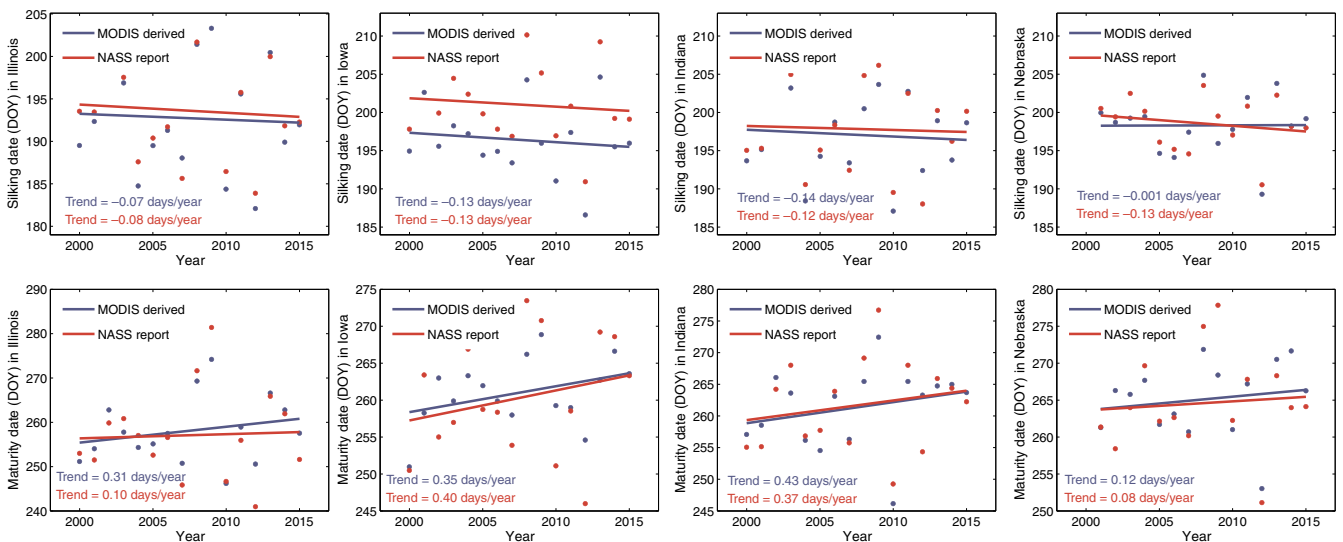


FIGURE 4 Time series of MODIS derived (blue) and NASS reported (red) silking and maturity date for four states during 2000-2015. The lines show the GFL trend estimated by the nonparametric Theil-Sen fitting

which is also based on NASS report, this empirical estimation solely based on NASS report suggests GFP prolongation contributed $31 \pm 4.8\%$ of the maize yield trend, which is slightly higher than the above estimation based on satellite data analysis.

A previous study suggested the solar brightening during GFP is responsible for about 27% of the observed increase in US maize yield from 1984 to 2013 (Tollenaar et al., 2017). However, we did not find a significant increase in solar radiation across the four corn states considered during the study period when using the same solar

radiation dataset integrated over the grain filling period (Supporting Information Figure S6).

When counties were grouped based on whether their GFP has increased or not, counties where GFP increased showed on average higher increasing rates of GDD_{crit} (0.82% per year) and grain yield (1.5% per year) compared to the mean of all the counties (Figure 7b). According to the estimated β_1 , the mean increase in GFP for those counties is estimated to have contributed to $27 \pm 0.8\%$ ($\pm SE$) of the yield trend. Alternatively, counties with decreasing GFP trend,

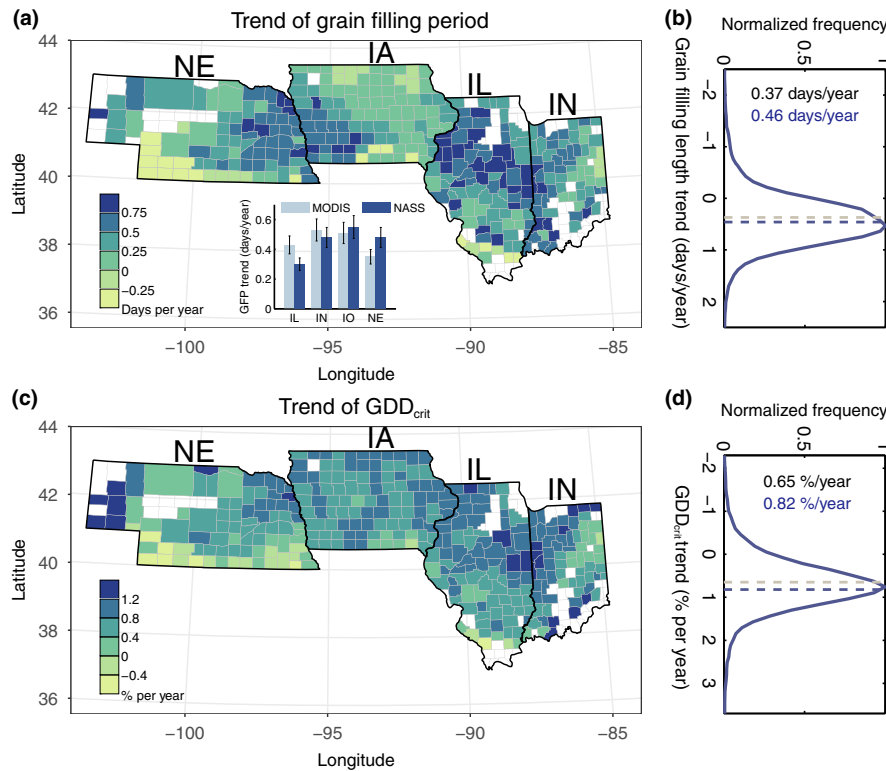


FIGURE 5 Trends in county-level grain filling length and grain filling GDD (GDD_{crit}), (a) and (c), where the empty counties mean that county has less than 12 years available data. For a specific year, a county with a number of maize grid cells less than 100 is regarded as unavailable. When estimating the trend, all of the grid cells in a county were pooled. And all of the trends shown are significant. The inset in (a) indicates GFP trend for the four states derived from NASS report and satellite data. The error bars indicate standard deviation of spatially estimated GFP trend. The distribution of grain filling length and GDD_{crit} trend in each 4 km grid, (b) and (d). The gray horizontal line illustrates the mean trend of GDD_{crit} or grain filling length for all counties and the blue horizontal line illustrates the mean trend of GDD_{crit} or grain filling length for the counties where GFP has extended. GFP is defined as the period from silking to maturity. The grain filling length and GDD_{crit} trend was estimated by the nonparametric Theil-Sen fitting

perhaps resulting from the effects of climatic warming overwhelming those of cultivars, showed a smaller yield trend of 1.0% per year (Figure 7b). Alternatively, when Equation 8 was applied to counties grouped by warmer and cooler growing season mean temperature separately, a significant ($p < 0.01$) lower yield benefit (β_1) was found in warmer counties (Figure 7b). This result implies that the yield benefit of GFP extension might be weakened in future warmer climate. This analysis also explained why the yield benefit in GFP prolonged counties was higher than the one estimated in GFP shortened counties (Figure 7b), since these counties generally have a warmer background climate (Supporting Information Figure S8).

To account for possible omitted variables in the above analysis, for instance, if an unobserved factor such as pest resistance affects both GFP and yield on a year-to-year basis, we also conducted a regression comparing linear yield trends with GFP trends over the study period as follows:

$$\text{yield trend}_i = \beta_1 * \text{GFP trend}_i + \varepsilon_i \quad (9)$$

where i is the county indices. In this model, the effect of year-to-year variation in each county is minimized, thus the significant slope (0.82% per day) primarily quantifies the contribution of GFP trend to yield trend (Figure 7c), which was close to the one of the panel

analysis (0.86% per day). The intercept term in this regression (1.1% per years) indicates the yield trend with no GFP extension and is 27% lower than the trends of GFP extended counties (1.5% per year), which is also consistent with the above estimation.

To further guard against the impact of potential confounding factors which might be not fully separated in the statistical models, the process-based crop model APSIM was then applied to simulate the contribution of GFP extension to yield trend. In this analysis, the variety GDD_{crit} parameter of the model was increased to simulate the observed variety shift caused GFP extension. Three simulations were conducted: sim1 has no increase in GDD_{crit} ; sim2 assumes an increase GDD_{crit} of 0.65% per year from the observed mean GDD_{crit} trend in all counties; sim3 sets a larger increase in GDD_{crit} of 0.82% per year consistent with observed mean GDD_{crit} trend over a subset of counties showing significant GFP increase. Compared to the results of sim1, the modeled increasing trends of GFP in sim2 and sim3 were close to the observed GFP trend (Figure 8). The yield increase in sim2 and sim3 attributable to GDD_{crit} presents a positive trend of 0.24% and 0.34% per year, respectively (Figure 9), which thus produces a close estimation of the contribution of GFP extension to yield trend (Table 2). The results from sim1 also confirm that the GFP extension was caused by shift in varieties because the GFP

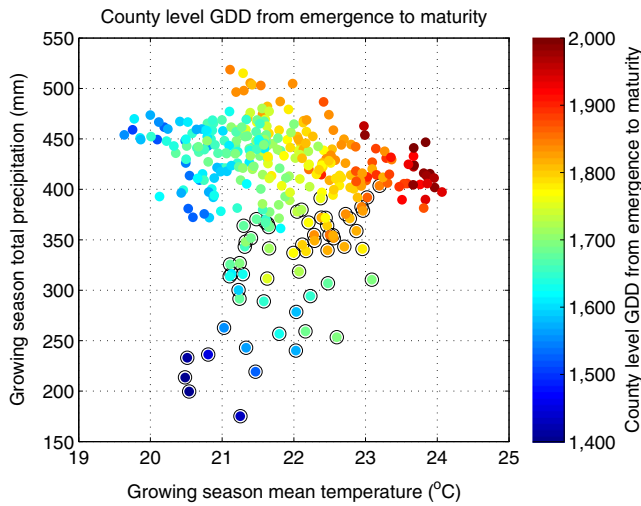


FIGURE 6 Scattering of county level (332 counties) multiple year mean GDD from emergence to maturity in temperature and precipitation space (points with black circles indicate the counties with irrigated area >50%)

is shortened by climatic warming where there is no increase in variety GDD_{crit} (Figure 8).

Climate change is also expected to exacerbate the variability of crop yields (Ray, Gerber, Macdonald, & West, 2015; Wheeler & von Braun, 2013). Therefore, we analyzed the influence of a prolonged GFP on yield stability, another important dimension of food security (Campbell et al., 2016). We used the coefficient of variation (CV) of yield in each county during 2000–2015 as an index of stability. A generalized additive regression model (GAM), suitable to account for nonlinear effects of explanatory variables, was employed to relate yield CV with GFP. We found that a longer GFP (Figure 10a) and an increase of GFP over time (Figure 10b) correspond to lower CV of yield when accounting for the climatic covariates, suggesting that longer GFP in both space and time is associated with more stable yields. The reason might be that the selection of longer GFP cultivars is associated with increasing stress tolerance and thereby reduces the negative impact of warming on yield stability (Tollenaar & Lee, 2002).

Finally, the APSIM model was used to investigate the future benefit of maize production across the US Midwest with three ensembles of future climate forcing data to account for the climate model uncertainty in global temperature. The simulations for the next 50 years suggest that if farmers are able to switch to longer maturity variety (at the GDD_{crit} current rate of 0.82% per year), the maize GFP in 2060–2070 will be lengthened by 25% and 18% under the RCP 2.6 and RCP 6.0 (Figure 11a), respectively. This means an approximate 15 days extension of GFP under the RCP 2.6, so the future maturity date still falls in a reasonable period for harvesting in these simulations. Simulations indicate that a continuation of the GFP prolongation rate would continue to benefit yields (Figure 11b), albeit by a smaller amount in future climate conditions compared to the historic period (Figure 11c). Specifically, the predicted 10.8% and

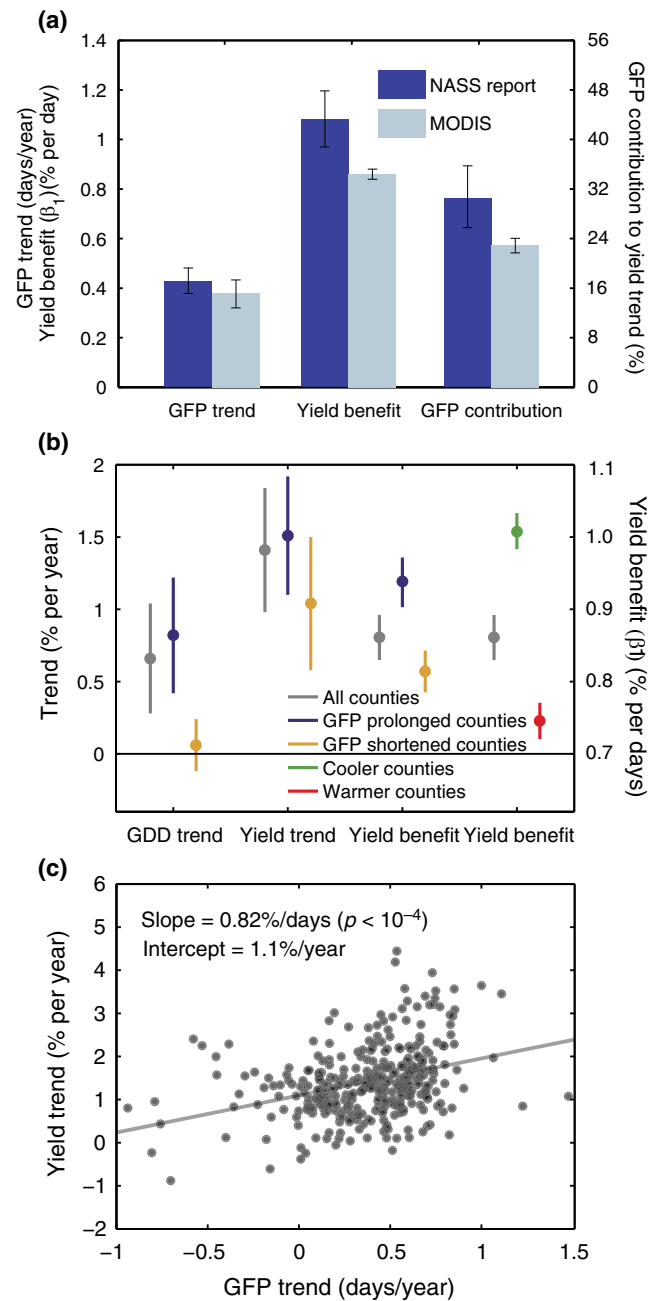


FIGURE 7 GFP trend, yield benefit of GFP prolongation and contribution of GFP prolongation to yield increase. (a) GFP trend, yield benefit (β_1) and GFP contribution to yield increase estimated from NASS report and MODIS-derived maize phenological progress data. GFP contribution was computed as: $\beta_1 \times$ GFP increasing trend/Yield increasing trend. The scales for GFP contribution to yield increase are shown in right y-axis. (b) GDD_{crit} trend, yield trend and yield benefit of GFP extension (β_1) based on counties grouped by whether their GFP have prolonged or not. Yield benefit was also separately estimated by grouping growing season mean temperature. Warmer and cooler counties were divided according to the median value of growing season mean temperature. The yield benefit is then estimated by applying Equation 8 to each group. The scales for yield benefit are shown in right y-axis. The error bars in (a) and (b) indicate the SD of each estimation. (c) The effect of GFP trend on maize yield trend. Each point corresponds to one county's trend in GFP and yield during 2000–2015

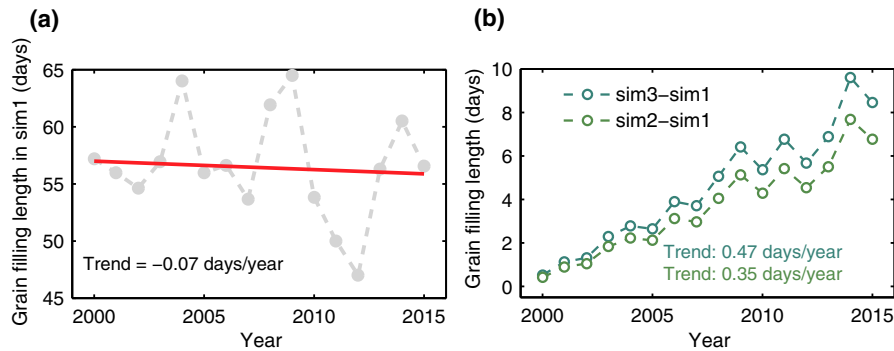


FIGURE 8 Simulated grain filling length to explore the contribution of grain filling length to the growing maize yield using APSIM 7.7. sim1 is the control without grain filling prolongation; sim2 is to increase GDD_{crit} by 0.65% per year to characterize the observed GDD_{crit} trend in all counties; sim3 is to increase GDD_{crit} by 0.82% per year to characterize observation of GFP prolonged counties. The left panel shows the mean time series of GFL in simulation 1 and the right panel shows the GFL difference

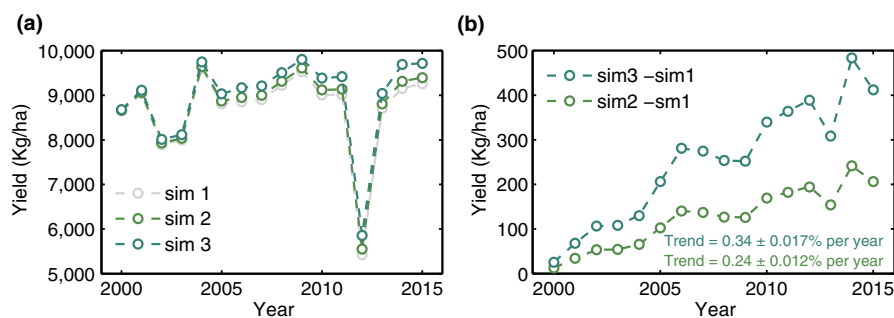


FIGURE 9 APSIM 7.7 simulated maize grain yield with different rate of GFP prolongation to explore the contribution of grain filling length to growing maize yield

TABLE 2 Contribution of grain filling length extension to the maize yield increasing trend estimated using APSIM (\pm indicates the SE)

	GFP prolonged counties	All counties
GDDcrit increasing rate (% per year)	0.82	0.65
Simulated yield increase rate (% per year)	0.34	0.24
Observed yield trend (% per year)	1.5 ± 0.07	1.4 ± 0.08
Contribution	$23 \pm 1.6\%$	$17 \pm 1.1\%$

13.6% yield loss under RCP 2.6 and RCP 6.0 could be partially offset by longer GFP, with a benefit of 7.2% and 5.6% under RCP 2.6 and RCP 6.0, respectively. The reduced benefit of GFP results in part from the increasing water and heat stress under a future warmer climate (Supporting Information Figure S9), which could decrease yield significantly during maize grain formation (Siebers et al., 2017).

Overall, we found there was a significant GFP extension and concurrent increasing GDD_{crit} during the last 16 years across the US Midwest Corn Belt, which is likely to reflect changes in the traits of maize cultivars. The GFP prolongation shows the potential to increase the maize yield and also to stabilize the yield variability but its yield benefit might diminish under future warmer climate. Although the GFP

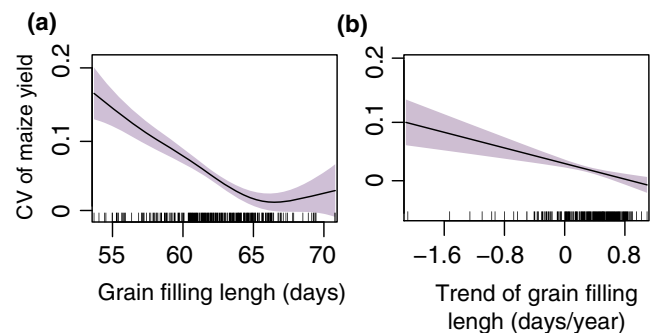


FIGURE 10 The effect of grain filling length on maize yield stability. Coefficient of variation (CV) of the yield in each county over 2000–2015 as a function of (a) the multiyear mean grain filling length, and (b) the trend of the grain filling period. Both longer GFP across different counties in space (a) and time (b) are associated with a smaller CV of yield, that is, more stable yields. The shaded areas indicate the 95% confidence interval. Each small bar next to the horizontal line is a value observed for a county

information extracted here is mainly based on satellite observed canopy chlorophyll content but not on ground identified kernel color development, this method estimated a similar GFP trend and contribution of GFP prolongation to yield increase across the US Midwest when compared with the state level statistical data and more

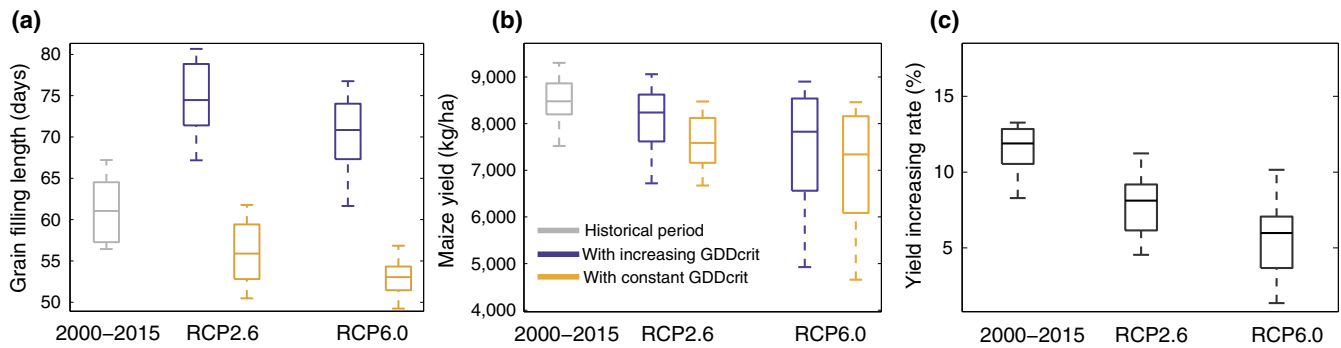


FIGURE 11 The benefit of prolonged grain filling period for maize yield in future climate. Boxplot of grain filling length (a) and maize yield (b) simulated with the APSIM model running up to 2060–2070 assuming constant (yellow) or linearly increasing GDD_{crit} at the same rate than during the past 16 years (blue) in comparison with the historic period 2000–2015. (c) Comparison of maize yield benefit with GDD_{crit} increase at the rate of 0.82% per year in historic and future climate conditions. Here yield increasing rate up to 2060–2070 is calculated by $(\text{yield with prolonged } GDD_{crit} - \text{yield with constant } GDD_{crit}) / (\text{yield with constant } GDD_{crit})$ using three climate forcing data: 2000–2015, RCP2.6, RCP6.0 (see Section 2). The lines in the middle of box represent median projection, boxes show the interquartile range, and whiskers indicate the 5th–95th percentile of projections

importantly it provided more detailed spatial information. Our study suggests that the historic satellite data can be utilized to map field crop phenological traits at large scales with fine spatial resolution to understand how farm management influence yield trend and the climatic response of crop growth at specific stage. When the observed GFP prolongation rate is applied up to 2070, the negative impact of climatic warming is partially offset by lengthening the GFP, but the grain yield still decreased even in the mild emission climate scenario, highlighting multiple adaptation strategies are necessary for future agricultural management in the region.

ACKNOWLEDGMENTS

We thank two anonymous reviewers' comments to help us significantly improve this study. This research was supported by a NSF project (IIS-1027955) and a NASA LCLUC project (NNX09AI26G) to Q. Z. We acknowledge the Rosen High Performance Computing Center at Purdue for computing support.

ORCID

Peng Zhu  <http://orcid.org/0000-0001-7835-3971>

Zhenong Jin  <http://orcid.org/0000-0002-1252-2514>

REFERENCES

- Abatzoglou, J. T. (2013). Development of gridded surface meteorological data for ecological applications and modelling. *International Journal of Climatology*, 33, 121–131. <https://doi.org/10.1002/joc.3413>
- Abendroth, L. J., Elmore, R. W., Boyer, M. J., & Marlay, S. K. (2011). *Corn growth and development*. Ames, IA: Iowa State University Extension.
- Badu-Apraku, B., Hunter, R. B., & Tollenaar, M. (1983). Effect of temperature during grain filling on whole plant and grain yield in maize (*Zea mays* L.). *Canadian Journal of Plant Science*, 63, 357–363. <https://doi.org/10.4141/cjps83-040>
- Çakir, R. (2004). Effect of water stress at different development stages on vegetative and reproductive growth of corn. *Field Crops Research*, 89, 1–16.
- Campbell, B. M., Vermeulen, S. J., Aggarwal, P. K., Corner-Dolloff, C., Girvetz, E., Loboguerrero, A. M., ... Wollenberg, E. (2016). Reducing risks to food security from climate change. *Global Food Security*, 11, 34–43. <https://doi.org/10.1016/j.gfs.2016.06.002>
- Cheikh, N., & Jones, R. J. (1994). Disruption of maize kernel growth and development by heat stress (Role of Cytokinin/Abcisic Acid Balance). *Plant Physiology*, 106, 45–51. <https://doi.org/10.1104/pp.106.1.45>
- Crafts-Brandner, S. J. (2002). Sensitivity of photosynthesis in a C4 plant, maize, to heat stress. *Plant Physiology*, 129, 1773–1780. <https://doi.org/10.1104/pp.002170>
- Crosbie, T. M., & Mock, J. J. (1981). Changes in physiological traits associated with grain yield improvement in three maize breeding programs. *Crop Science*, 21, 255–259. <https://doi.org/10.2135/cropsci1981.0011183X002100020013x>
- Daly, C., Halbleib, M., Smith, J. I., Gibson, W. P., Doggett, M. K., Taylor, G. H., ... Pasteris, P. P. (2008). Physiographically sensitive mapping of climatological temperature and precipitation across the conterminous United States. *International Journal of Climatology*, 28, 2031–2064. <https://doi.org/10.1002/joc.1688>
- Driedonks, N., Rieu, I., & Vriezen, W. H. (2016). Breeding for plant heat tolerance at vegetative and reproductive stages. *Plant Reproduction*, 29, 67–79. <https://doi.org/10.1007/s00497-016-0275-9>
- Duvick, D. N. (2005). The contribution of breeding to yield advances in maize (*Zea mays* L.). *Advances in Agronomy*, 86, 83–145. [https://doi.org/10.1016/S0065-2113\(05\)86002-X](https://doi.org/10.1016/S0065-2113(05)86002-X)
- Dwyer, L. M., Ma, B. L., Evenson, L., & Hamilton, R. I. (1994). Maize physiological traits related to grain yield and harvest moisture in mid-to short-season environments. *Crop Science*, 34, 985–992. <https://doi.org/10.2135/cropsci1994.0011183X003400040029x>
- Egli, D. B. (2004). Seed-fill duration and yield of grain crops. *Advances in Agronomy*, 83, 243–279. [https://doi.org/10.1016/S0065-2113\(04\)83005-0](https://doi.org/10.1016/S0065-2113(04)83005-0)
- Gitelson, A. A. (2004). Wide dynamic range vegetation index for remote quantification of biophysical characteristics of vegetation. *Journal of Plant Physiology*, 161, 165–173. <https://doi.org/10.1078/0176-1617-01176>
- Gitelson, A. A., Schalles, J. F., & Hladik, C. M. (2007). Remote chlorophyll-a retrieval in turbid, productive estuaries: chesapeake Bay case study. *Remote Sensing of Environment*, 109, 464–472. <https://doi.org/10.1016/j.rse.2007.01.016>

- Guindin-Garcia, N., Gitelson, A. A., Arkebauer, T. J., Shanahan, J., & Weiss, A. (2012). An evaluation of MODIS 8- and 16-day composite products for monitoring maize green leaf area index. *Agricultural and Forest Meteorology*, *161*, 15–25. <https://doi.org/10.1016/j.agrformet.2012.03.012>
- Hammer, G. L., Van Oosterom, E., McLean, G., Chapman, S. C., Broad, I., Harland, P., & Muchow, R. C. (2010). Adapting APSIM to model the physiology and genetics of complex adaptive traits in field crops. *Journal of Experimental Botany*, *61*, 2185–2202. <https://doi.org/10.1093/jxb/erq095>
- Holzworth, D. P., Huth, N. I., deVoil, P. G., Zurcher, E. J., Herrmann, N. I., McLean, G., ... Keating, B. A. (2014). APSIM – Evolution towards a new generation of agricultural systems simulation. *Environmental Modelling & Software*, *62*, 327–350. <https://doi.org/10.1016/j.envsoft.2014.07.009>
- Huete, A., Didan, K., Miura, T., Rodriguez, E. P., Gao, X., & Ferreira, L. G. (2002). Overview of the radiometric and biophysical performance of the MODIS vegetation indices. *Remote Sensing of Environment*, *83*, 195–213. [https://doi.org/10.1016/S0034-4257\(02\)00096-2](https://doi.org/10.1016/S0034-4257(02)00096-2)
- Irmak, S., Haman, D. Z., & Bastug, R. (2000). Determination of crop water stress index for irrigation timing and yield estimation of corn. *Agronomy Journal*, *92*, 1221–1227. <https://doi.org/10.2134/agronj2000.9261221x>
- Jin, Z., Ainsworth, E. A., Leakey, A. D. B., & Lobell, D. B. (2018). Increasing drought and diminishing benefits of elevated carbon dioxide for soybean yields across the US Midwest. *Global Change Biology*, *24*, e522–e533. <https://doi.org/10.1111/gcb.13946>
- Keenan, T. F., Gray, J., Friedl, M. A., Toomey, M., Bohrer, G., Hollinger, D. Y., ... Richardson, A. D. (2014). Net carbon uptake has increased through warming-induced changes in temperate forest phenology. *Nature Climate Change*, *4*, 598–604. <https://doi.org/10.1038/nclimate2253>
- Kiniry, J. R., & Bonhomme, R. (1991). Predicting crop phenology, *11*, 5–131.
- Lobell, D. B., & Field, C. B. (2008). Estimation of the carbon dioxide (CO₂) fertilization effect using growth rate anomalies of CO₂ and crop yields since 1961. *Global Change Biology*, *14*, 39–45.
- Lobell, D. B., Hammer, G. L., McLean, G., Messina, C., Roberts, M. J., & Schlenker, W. (2013). The critical role of extreme heat for maize production in the United States. *Nature Climate Change*, *3*, 497–501. <https://doi.org/10.1038/nclimate1832>
- Lobell, D. B., Roberts, M. J., Schlenker, W., Braun, N., Little, B. B., Rejesus, R. M., & Hammer, G. L. (2014). Greater sensitivity to drought accompanies maize yield increase in the U.S. Midwest. *Science*, *344*, 516–519.
- McMaster, G. S. (2005). Phytomers, phyllochrons, phenology and temperate cereal development. *Journal of Agricultural Science*, *143*, 137–150. <https://doi.org/10.1017/S0021859605005083>
- Meinshausen, M., Smith, S. J., Calvin, K., Daniel, J. S., Kainuma, M. L. T., Lamarque, J.-F., ... van Vuuren, D. P. P. (2011). The RCP greenhouse gas concentrations and their extensions from 1765 to 2300. *Climatic Change*, *109*, 213–241. <https://doi.org/10.1007/s10584-011-0156-z>
- Mitchell, K. E. (2004). The multiinstitution North American Land Data Assimilation System (NLDAS): utilizing multiple GCIP products and partners in a continental distributed hydrological modeling system. *Journal of Geophysical Research*, *109*, D07S90.
- National Research Council (2010) *The impact of genetically engineered crops on farm sustainability in the United States*. Washington, DC: National Academies Press.
- Porter, J. R., & Semenov, M. A. (2005). Crop responses to climatic variation. *Philosophical Transactions of the Royal Society B-Biological Sciences*, *360*, 2021–2035. <https://doi.org/10.1098/rstb.2005.1752>
- Rattalino Edreira, J. I., & Otegui, M. E. (2013). Heat stress in temperate and tropical maize hybrids: a novel approach for assessing sources of kernel loss in field conditions. *Field Crops Research*, *142*, 58–67. <https://doi.org/10.1016/j.fcr.2012.11.009>
- Ray, D. K., Gerber, J. S., Macdonald, G. K., & West, P. C. (2015). Climate variation explains a third of global crop yield variability. *Nature Communications*, *6*, 5989. <https://doi.org/10.1038/ncomms6989>
- Sacks, W. J., Deryng, D., Foley, J. A., & Ramankutty, N. (2010). Crop planting dates: an analysis of global patterns. *Global Ecology and Biogeography*, *19*, 607–620.
- Sacks, W. J., & Kucharik, C. J. (2011). Crop management and phenology trends in the U.S. Corn Belt: impacts on yields, evapotranspiration and energy balance. *Agricultural and Forest Meteorology*, *151*, 882–894. <https://doi.org/10.1016/j.agrformet.2011.02.010>
- Sakamoto, T., Gitelson, A. A., & Arkebauer, T. J. (2014). Near real-time prediction of U.S. corn yields based on time-series MODIS data. *Remote Sensing of Environment*, *147*, 219–231. <https://doi.org/10.1016/j.rse.2014.03.008>
- Sakamoto, T., Wardlow, B. D., Gitelson, A. A., Verma, S. B., Suyker, A. E., & Arkebauer, T. J. (2010). A Two-Step Filtering approach for detecting maize and soybean phenology with time-series MODIS data. *Remote Sensing of Environment*, *114*, 2146–2159. <https://doi.org/10.1016/j.rse.2010.04.019>
- Sánchez, B., Rasmussen, A., & Porter, J. R. (2014). Temperatures and the growth and development of maize and rice: a review. *Global Change Biology*, *20*, 408–417. <https://doi.org/10.1111/gcb.12389>
- Schlenker, W., & Roberts, M. J. (2009). Nonlinear temperature effects indicate severe damages to U.S. crop yields under climate change. *Proceedings of the National Academy of Sciences*, *106*, 15594–15598. <https://doi.org/10.1073/pnas.0906865106>
- Siebers, M. H., Slattery, R. A., Yendrek, C. R., Locke, A. M., Drag, D., Ainsworth, E. A., ... Ort, D. R. (2017). Simulated heat waves during maize reproductive stages alter reproductive growth but have no lasting effect when applied during vegetative stages. *Agriculture, Ecosystems and Environment*, *240*, 162–170. <https://doi.org/10.1016/j.agee.2016.11.008>
- Siebers, M. H., Yendrek, C. R., Drag, D., Locke, A. M., Rios Acosta, L., Leakey, A. D., ... Ort, D. R. (2015). Heat waves imposed during early pod development in soybean (*Glycine max*) cause significant yield loss despite a rapid recovery from oxidative stress. *Global Change Biology*, *21*, 3114–3125. <https://doi.org/10.1111/gcb.12935>
- Thomas, H., & Ougham, H. (2014). The stay-green trait. *Journal of Experimental Botany*, *65*, 3889–3900. <https://doi.org/10.1093/jxb/eru037>
- Tollenaar, M., Fridgen, J., Tyagi, P., Stackhouse, P. W., & Kumudini, S. (2017). The contribution of solar brightening to the US maize yield trend. *Nature Climate Change*, *7*, 275–278. <https://doi.org/10.1038/nclimate3234>
- Tollenaar, M., & Lee, E. A. (2002). Yield potential, yield stability and stress tolerance in maize. *Field Crops Research*, *75*, 161–169. [https://doi.org/10.1016/S0378-4290\(02\)00024-2](https://doi.org/10.1016/S0378-4290(02)00024-2)
- Tollenaar, M., & Wu, J. (1999). Yield improvement in temperate maize is attributable to greater stress tolerance. *Crop Science*, *39*, 1597–1604. <https://doi.org/10.2135/cropsci1999.3961597x>
- USDA (2015) *World Agricultural Supply and Demand Estimates* (pp. 1–40). Washington, DC: United States Department of Agriculture.
- Vermote, E. F., & Vermeulen, A. (1999). Atmospheric correction algorithm: spectral reflectances (MOD09). ATBD version 4(April):1–107.
- Wang, G., Kang, M. S., & Moreno, O. (1999). Genetic analyses of grain-filling rate and duration in maize. *Field Crops Research*, *61*, 211–222. [https://doi.org/10.1016/S0378-4290\(98\)00163-4](https://doi.org/10.1016/S0378-4290(98)00163-4)
- Wheeler, T., & von Braun, J. (2013). Climate change impacts on global food security. *Science*, *341*, 508–513. <https://doi.org/10.1126/science.1239402>
- Wood, S. N. (2006). Generalized additive models: an introduction with R. *Texts Stat. Sci.* xvii, 392.
- Zeng, L., Wardlow, B. D., Wang, R., Shan, J., Tadesse, T., Hayes, M. J., & Li, D. (2016). A hybrid approach for detecting corn and soybean

phenology with time-series MODIS data. *Remote Sensing of Environment*, 181, 237–250. <https://doi.org/10.1016/j.rse.2016.03.039>

SUPPORTING INFORMATION

Additional supporting information may be found online in the Supporting Information section at the end of the article.

How to cite this article: Zhu P, Jin Z, Zhuang Q, et al. The important but weakening maize yield benefit of grain filling prolongation in the US Midwest. *Glob Change Biol.* 2018;00:1–13. <https://doi.org/10.1111/gcb.14356>